Periodica Polytechnica
Mechanical Engineering

59(2), pp. 51-59, 2015
DOI: 10.3311/PPme.7780


# Wear Measurement on Chain Joint Components Using a Roundness Instrument

Daniel Sappok[1 *], Bernd Sauer[1]

RESEARCH ARTICLE

Received 23 October 2014; accepted after revision 16 January 2015

***Abstract***

*Driving and timing chains are widely used machine elements which are continuously improved regarding wear and energy efficiency. Especially for timing chains, reducing wear is of high importance as the chain is critical for the function of the combustion engine. To achieve this goal, the wear within the chain joint has to be measured precisely which is usually done by measuring the length of the entire chain. With this measurement, no information about the distribution of wear between the contacting bodies, pin and bush, is available. An additional measuring and analyzing technique using a standard roundness instrument is developed with which more detailed information about the wear within the chain joint is obtained. With this new method, unworn chain joint components are characterized and the wear on worn components is measured and compared for pins with different surface treatments. Furthermore, approaches to use the measured data in simulation and calculation are presented.*

***Keywords***

*chain drives, wear measurement, roundness measurement, wear calculation*

## 1 Introduction

The chain joint of driving and timing chains, which consists of a pin and a bush, is a very critical part as far as wear and energy efficiency is concerned. The joint wear of driving chains determines their lifetime. In an operating chain drive, the chain is loaded with a driving torque that leads to the contact forces within the chain joints. When the chain runs onto and off the sprocket, the two parts of the chain joints, perform a relative motion. The same occurs if there are vibrations in the slack strand of the chain drive. Due to the contact force and the sliding motion, the pin and the bush of the chain joints are worn out at a certain area which is shown in Fig. 1. The clearance of the joints is increased leading to an elongation of the entire chain.

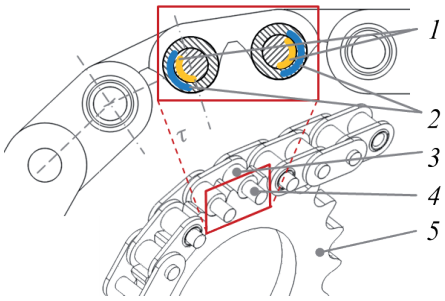


**Fig. 1** Areas of wear in bush chain joints (1: wear areas on pin; 2: wear areas on bush; 3: bush; 4: pin; 5: sprocket).

For example low-viscosity engine oils negatively influence this wear behavior of timing chains [1,2]. Thus, improving the wear behavior is necessary to realize approaches to optimize the energy efficiency of the whole engine. These include reducing the friction losses within the chain joint which determine to a large amount the energy efficiency of the entire chain [3].

Commonly used chain types for timing chain drives are bush and roller chains which are shown in Fig. 2.

To reduce wear and friction losses, different materials for pins and bushes and various surface treatments for both components are used and the tribological system is thus constantly improved. For the development of these optimizations, the performance of the chains is determined on chain test rigs as engine tests would be too costly in terms of time and money. These test rigs allow

[1] Institute of Machine Elements, Gears, and Transmissions (MEGT), University of Kaiserslautern, Germany

[*] Corresponding author, e-mail: daniel.sappok@mv.uni-kl.de

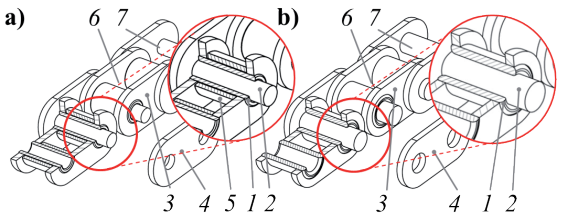


**Fig. 2** Configuration of roller (a) and bush (b) chains (1: bush; 2: pin; 3: inner plate; 4: outer plate; 5: roller; 6: inner link; 7: outer link)

for operating chains with well-defined conditions which are usually chosen to be as close as possible to the real application. The results from the test rig still have to be checked against results from engine tests to make sure that the conditions are comparable.

For these investigations, modular back to back test rigs for chain drives have been developed at the MEGT which allow for operating various types of chains and which are suitable for wear and energy efficiency investigation.

In addition, a wear calculation tool for roller and bush chains has been developed. It calculates the contact between pin and bush in dependency of the inner contour of the bush and the bending line of the pin. With the local contact pressure, the wear volume can be calculated on the basis of Archard's empirical wear model [4]. This allows for calculating the changed inner contour of the bush [5,6].

For both experiments and simulation, measuring wear on the chains is challenging. This is due to the fact that the worn surfaces are not accessible without disassembling the chains. For measuring the length of the chain, a normal load has to be applied to avoid a clearance in the chain joint. This load directly influences the length due to elastic deformation and thus has to be as reproducible as possible. Furthermore the amount of wear per chain joint is very low. For timing chains, the tolerable elongation is 0.3–0.5 %, which is 40 µm for a chain with a pitch of 8 mm. In order to get information on the running-in behavior, the wear elongation is measured multiple times during the test run. During these measurements it is of crucial importance that the wear behavior of the chain is not influenced when the test run is continued. To meet all these requirements, various methods for measuring wear were developed at the MEGT. These include an online wear measurement on the test rig, a clearance and stiffness measurement device and a length measurement device. All methods have different advantages and disadvantages but none of them is able to provide local information about the wear distribution on and between the components of the chain joint. Therefore a roundness measuring technique has been developed which is able to overcome this drawback.

In this paper, the experimental methods and simulation techniques that are used for chain wear investigations are presented. Furthermore, a self-developed technique for using the results from roundness measurements on a standard roundness instrument to gain further information about the wear behavior and to derive wear parameters for comparison between different components is presented. This method is then applied to new and worn chain components and a first approach to use the results as input data for a wear calculation model is described.

### 1.1 Experimental Investigations

To conduct wear investigations with operating conditions that are very close to the real situation in the application of the chain, a back to back wear test rig is used (Fig. 3). This test rig can be operated with different types of chains such as roller, bush and silent chains. Furthermore, the wear or the energy efficiency can be of interest for the investigation. To allow for this wide range of chain types and different tasks, the test rig is designed to be as modular as possible [7,8].

To apply the load torque on the chain, a mechanical tensioning clutch is used to tension two chains against each other. The rotation is applied with an electric engine. The load torque is measured with resistance strain gauges and the measurement data is transmitted with a telemetry system from the rotating shaft. With the constantly monitored load torque, the wear elongation for both chains is calculated online through the loss of load torque due to the elongation of the chain while taking the thermal expansion into account. Therefore, the temperature of the relevant components is measured and the thermal expansion is calculated with pre-determined coefficients of thermal expansion. A force-feed lubricant application is used and the lubricant can be tempered up to 100 °C in the lubricant supply unit.

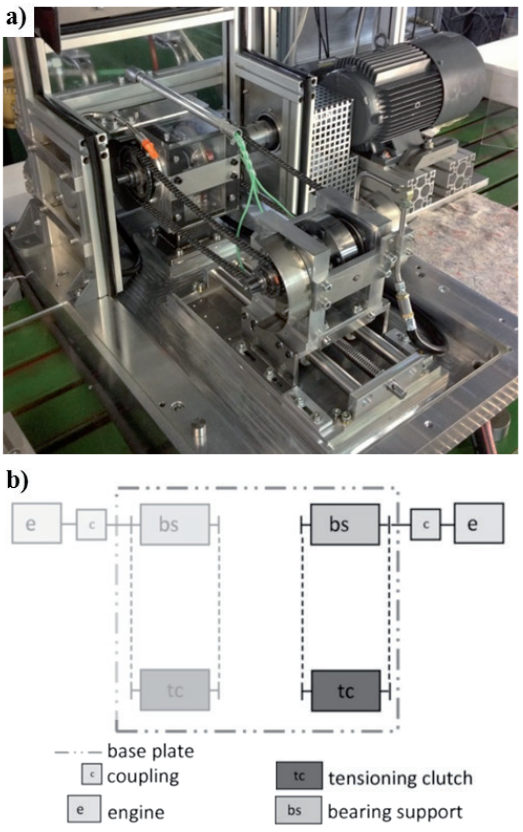


**Fig. 3** Experimental wear investigations: a) back to back wear test rig; b) schematic representation of the test rig showing the setup for wear investigations

The wear that occurs during the operation is measured with different methods. For example a length measurement unit and a clearance and stiffness measurement device are used (Fig. 4). With both devices, the wear elongation over the operating time of the chain is obtained from which the running-in wear during the first hours and the steady-state wear can be derived [7]. With both methods, the chain need not be disassembled or opened. The length measurement is very quick while the more complicated clearance and stiffness measurement provides additional information.

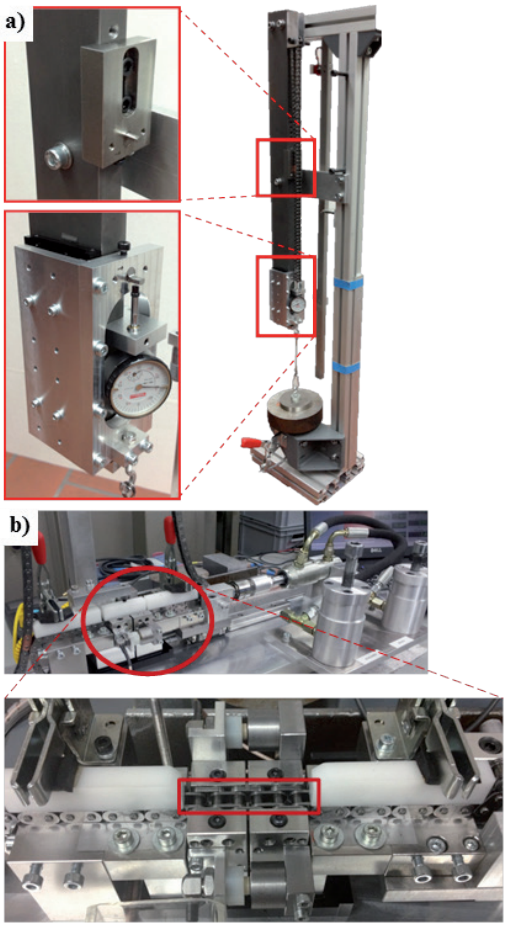


**Fig. 4** Wear measurement: a) length measurement device; b) clearance and stiffness measurement devices

Figure 5 shows two wear elongation curves that were obtained with the length measurement device. The tested chains are bush chains with a pitch of 8 mm. Both chains were operated in one test run with equal operating conditions but were equipped with different types of pins. Chain 1 was built of case-hardened 16MnCr5 pins and case-hardened 10NiCr5-4 bushes, both having almost the same surface hardness of 880-920 HV0.01. Chain 2 consists of inchromized Cr60e pins and the same case-hardened bushes as Chain 1. With a surface hardness of over 1400 HV0.01, these pins are much harder than the bushes.

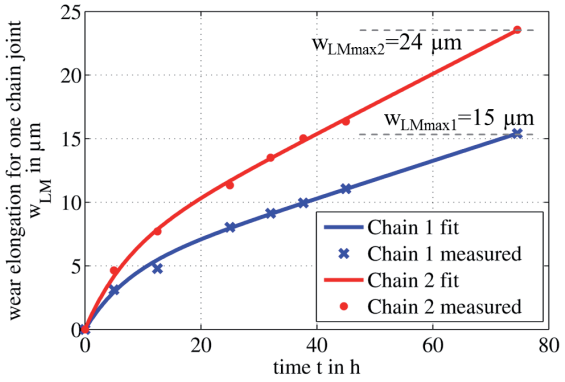


**Fig. 5** Wear elongation over time for two chains with different pins

The measured wear elongation at discrete runtimes was used to derive the running-in wear $w_0$, a running-in half-time $T_{ri}$ and the slope $k$ during steady-state wear. With these values, a fitted wear curve is calculated using Eq. (1) [9]:

$$w(t) = w_0 \cdot (1 - e^{-\ln(2)\ (t/Tri)}) + k \cdot t \qquad (1)$$

These results show that the length measurement can be used to determine the wear elongation and the behavior of the chains during the running-in period. This allows for comparing different chain types but further information about details of the wear on the chain components cannot be derived from the results. Therefore additional measurements have to be conducted.

## 1.2 Simulation and Calculation

To complement the experimental methods presented above, simulations are conducted to calculate the inner loads in a chain joint and the wear progress itself. In order to calculate wear, a model has been developed at the MEGT. The contact between pin and bush is calculated analytically which includes the evaluation of the bending line and the force distribution along the axis of the pin. The bending line depends on the material and the cross section of the pin as well as the inner contour of the bush. These boundary conditions are all taken into account in the calculation of the bending line. With these results, the contact pressure distribution can be computed. The principle of this calculation model is shown in Fig. 6.

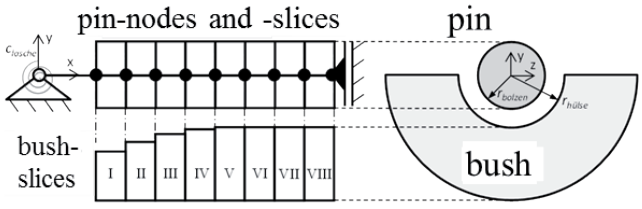


**Fig. 6** Schematic representation of the contact model with sliced pin and bush [5]

In the next step, a wear calculation approach is used. A commonly used approach is the one developed by Archard [4]. This approach with a wear coefficient $K$, contact force $F$ and the

sliding distance $s$ is modified to take the size of the contact area $A$ into account. Additionally, a non-linear influence of the contact force with the exponent $m$ can be included [10] which leads to the following equation:

$$V=K\cdot(F/A)^m\cdot s \tag{2}$$

With the calculated wear volume $V$, the new contact geometry can be computed. The quality of these results critically depends on the contact pressure distribution and the correctness of the load input data. To verify the contact pressure distribution, a finite-element model was developed in ABAQUS and the results of the wear calculation were compared to the FE simulation which showed a good correlation [5]. One limitation of this tool is that the wear volume and thus a change of the contour are completely applied to the bush. This assumption is valid for some chain types, depending on the type of materials and the surface treatment of pin and bush. For chain types where the pin also shows significant wear, this restriction has to be considered when interpreting the results. More details of the wear calculation model can be found in [5,6].

## 2 Roundness Measurement

As presented above, measuring the elongation of the whole chain or a part of the chain is an appropriate method to accompany the test runs as it is not necessary to disassemble the chain. But with this technique the distribution of wear between pin and bush cannot be determined. Figure 7 shows the cross section of the unworn shape of pin and bush and the material that is typically removed through wear.

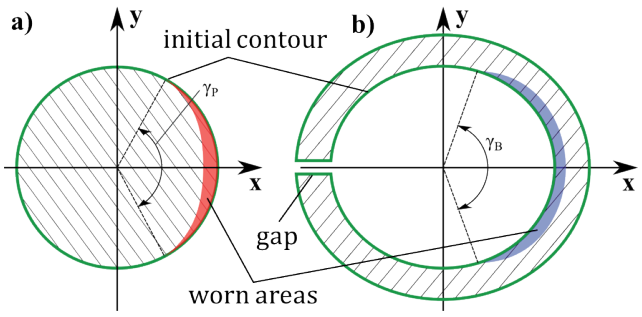


**Fig. 7** Worn areas on pin (a) and bush (b)

The pin (Fig. 7a) is ground which leads to an almost ideal circular shape. The bush (Fig. 7b) is rolled from sheet metal which leads to the gap opposite to the worn areas and the whole chain is stretched to its nominal pitch as a last step of the manufacturing procedure. This leads to the elliptical shape of the bush. To evaluate the size of the worn areas shown in Fig. 7, further measurements are necessary which involve disassembling the chain joint. This means that the measurements cannot be conducted during the test run.

When the chain joint is disassembled, the surface of the pin (Fig. 8) is easily accessible which allows for using various tactile and optical measurement techniques like stylus methods and confocal or white light microscopy.

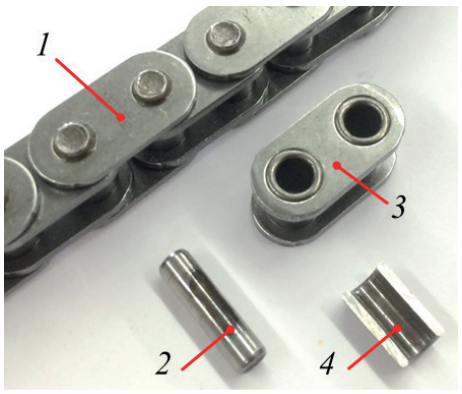


**Fig. 8** Chain joint components after disassembling (1: whole chain; 2: pin; 3: inner link; 4: opened bush)

But if these techniques are applied to the bush, it has to be opened to access the worn surface. As the bush is pressed into the plates, removing it would lead to an elastic deformation which could be in the same magnitude as the wear itself and would thus lead to wrong measurement results. Furthermore, the opened bush doesn't have unworn reference areas contrary to the pin where unworn areas in the axial direction and around the circumference exist. To overcome these problems, a measurement technique is necessary which can be applied to the closed bush. The roundness measurement is a tactile technique which can be used for this task.

### 2.1 Roundness Instrument

During measurement, the change in radius is gathered around the circumference on a cross section of a cylindrical body. This measurement can be repeated on different levels of a cylindrical sample to gain information about the cylindricity (see Fig. 9).

There are different strategies for measuring the cylindricity of a sample, like the bird-cage extraction, roundness profile extraction, generatrix extraction and the points extraction strategy which are all described in ISO 12180-2 [11]. The method that is used for the presented measurement procedure is the roundness profile extraction which is recommended when a high information quality on the roundness of the sample is needed [11].

The roundness measurement works as follows. The component is rotated on a highly accurate spindle (see Fig. 10). During the rotation, a transducer measures radial variations of the sample with respect to the spindle axis. Therefore the sample axis has to be aligned with the axis of the spindle which is done by means of a centering and leveling table.

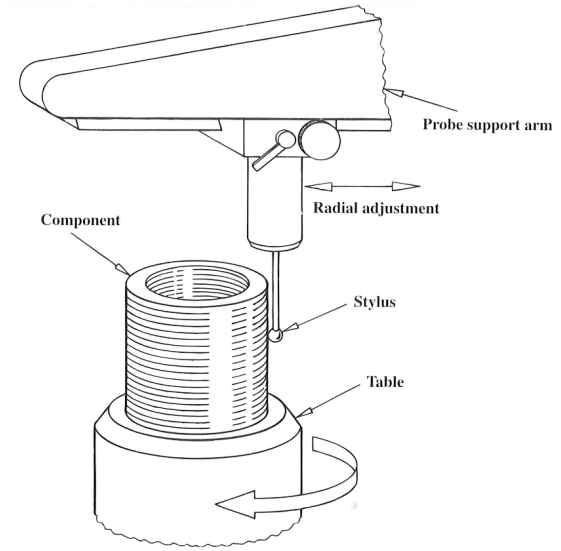


**Fig. 9** Principle of roundness measurement with turntable type of instrument [12]

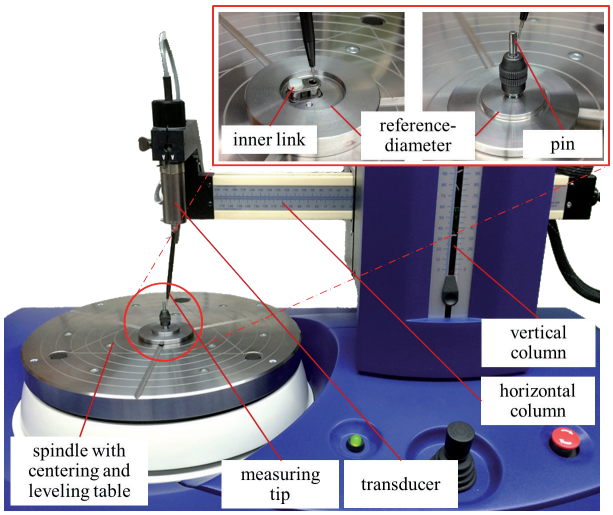


**Fig. 10** Roundness instrument with adapters for pin and bush (inner link)

The roundness instrument which is used for these investigations is a Talyrond 365 from Taylor Hobson which features a frictionless air bearing spindle and high accuracy columns. The centering and leveling table works automatically while this procedure requires two reference planes. These reference planes are available on the pin in the unworn areas (see Fig. 11) but not on the bush.

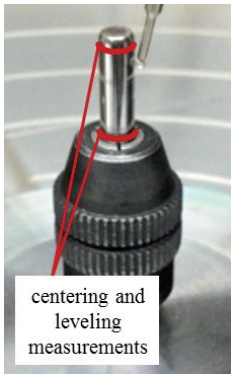


**Fig. 11** Centering and leveling planes in unworn areas of the pin

For the bush, the reference planes for centering and leveling are in worn areas so it is very likely that an eccentricity or tilt error remains which has to be taken into account when evaluating the results which is described later.

## 2.2 Setup

In order to position and fix the samples on the table of the roundness instrument, adapters were developed (see also Fig. 10). These adapters already ensure a reasonable alignment of the sample axis with the spindle axis which speeds up and improves the result of the centering and leveling procedure. The diameter of the samples cannot be determined directly as the roundness is measured independent of the diameter of the sample. To overcome this drawback, both adapters are equipped with a reference surface with 30 mm diameter. This reference surface is always measured prior to the actual surfaces and the coordinate system is calibrated through this measurement. Therefore, absolute values for radius or diameter can be measured additionally to the roundness but with limited accuracy. The resolution of the transducer is 0.03 µm and the accuracy of the diameter measurement when using a 30 mm reference diameter is ±3 µm.

## 2.3 Measuring Procedure and Data Processing

To ensure a high reproducibility, the measuring procedure is automated for pin and bush and a guideline has been developed for cleaning and mounting the samples. During each measurement, the sample is first centered and leveled. After that, the reference diameters with 30 mm are measured to set the reference diameter for the evaluation of absolute values. During the actual measurement, 20 equidistant roundness measurements are conducted for the pin and the bush along their axis. The obtained data is processed in the measurement software and externally in a self-developed MATLAB script. The process chart for the post-processing is shown in Fig. 12.

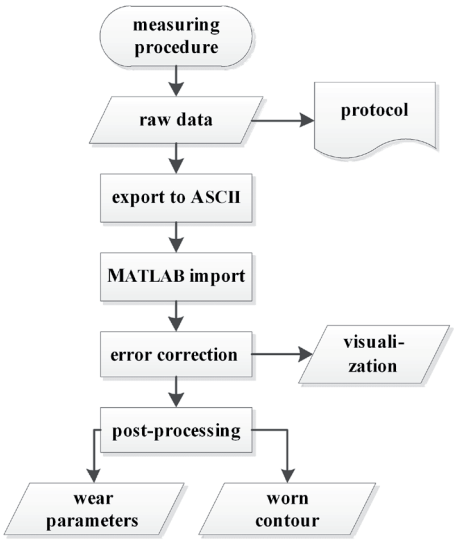


**Fig. 12** Process chart for the measurement and post-processing of the chain components

The raw data which is generated during the measuring procedure is processed to generate a protocol which includes standard roundness parameters like roundness total, roundness peak or roundness valley which are all based on deviations from reference circles. As the software is designed for quality management and production measurements, further post-processing, which is necessary to measure the size of the worn areas for example, is not possible. Therefore, the raw data is exported into the ASCII format and a self-developed MATLAB routine is used for the post-processing.

### 2.4 Post-Processing

The ASCII raw data is imported in MATLAB and converted into a cylindrical and a cartesian coordinate system. During the following steps, both coordinate systems are used depending on the kind of operation that is conducted. Fig. 13 shows the Cartesian (x,y,z) and the cylindrical (φ, r, z) coordinate system.

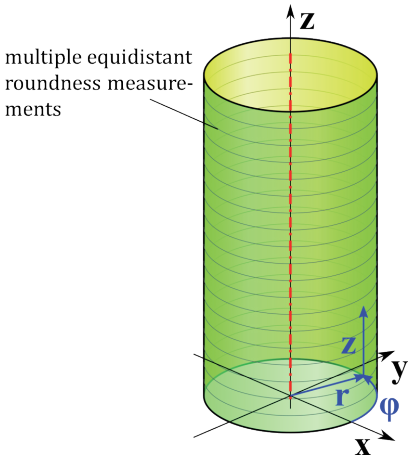


**Fig. 13** Definition of the cartesian (x,y,z) and the cylindrical (φ,r,z)coordinate systems

As already mentioned, the samples have to be centered and leveled which is already done during the measurement. But especially for the bush, a tilt error is still present in the measurement data. To remove this error, the contour of the sample is evaluated in +90° and -90° for pin and bush, and additionally in 180° for the pin (see Fig. 14a). From these contours, the slopes $m_1$, $m_2$, $m_3$ (see Fig. 14b-c) are calculated using a linear fit. With these slopes, correction factors for the tilt around the x- and y-axis are calculated and are applied to the measurement data leading to the corrected data shown in Fig. 14d.

The next steps are conducted on the corrected data. To obtain the unworn diameters of bush and pin for every measurement plane, a circle fit is applied to the measurement data. To avoid an influence of the wear on the result, only certain sections around the circumference are taken into account for the circle fit. These sections are shown in Fig. 15. Depending on the chain type and the chain drive layout, these sections have to be adjusted to be always outside the worn areas which are described by the wear angles $\gamma_P$ and $\gamma_B$.

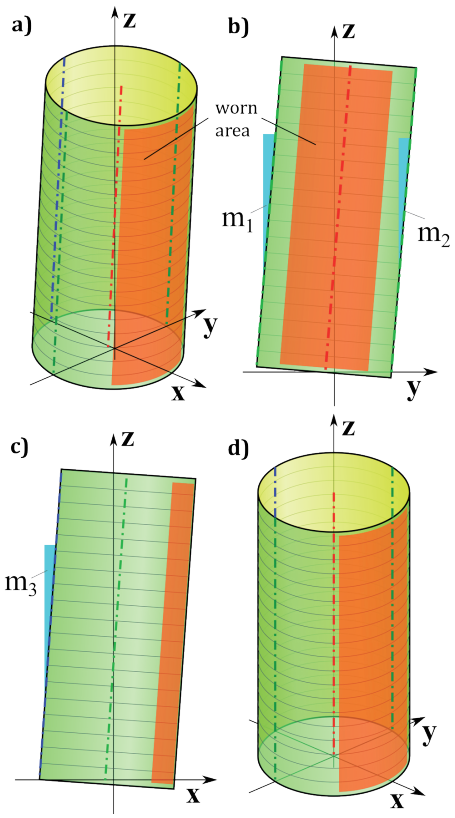


**Fig. 14** Removing tilt from measured data: a) raw measurement data; b) tilt correction around x-axis; c) tilt correction around y-axis; d) corrected data

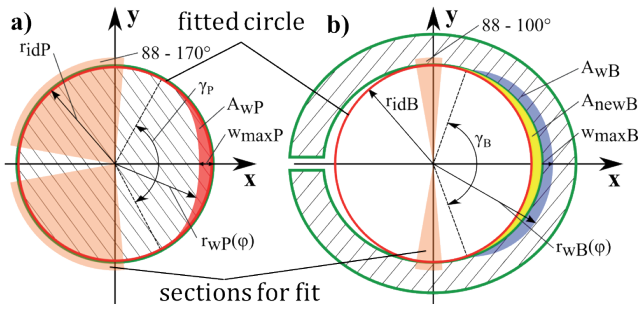


**Fig. 15** Definition of linear wear values and size of wear areas on pin (a) and bush (b)

The resulting diameters of the circle fit are used to check for the plausibility of the data and as a reference for the change of the shape due to wear. The center of the fitted circle is used to remove the remaining eccentricity of the cylinder. With the reference radii $r_{idP}$ and $r_{idB}$, the maximum linear wear values $w_{maxP}$ and $w_{maxB}$ are calculated from the measured data $r_{wP}(\varphi)$ and $r_{wB}(\varphi)$ using Eq. (3) and Eq. (4).

$$w_{maxP} = r_{idP} - min(r_{wP}(\varphi)) \tag{3}$$

$$w_{maxB} = max(r_{wB}(\varphi)) - r_{idB} \tag{4}$$

For the worn radii $r_{wP}(\varphi)$ and $r_{wB}(\varphi)$, only the areas where wear is expected are taken into account. The sizes of the worn areas $A_{wP}$ and $A_{wB}$ are also calculated which can be used to obtain the wear volumes $V_{wP}$ and $V_{wB}$ with the distance between the measurement planes.

Besides the wear values, the change of the axial contour of pin and bush is of high interest, which is evaluated at φ=0°, that is in the direction of the normal load when the chain joint is not deflected. The resulting contours are exemplary shown in Fig. 16.

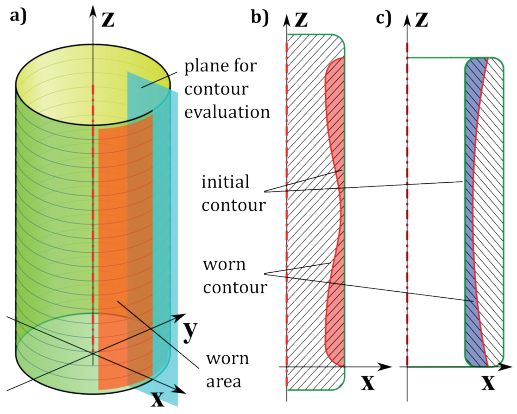


**Fig. 16** Contour evaluation on plane at φ=0° (a) with examplary initial and worn contours of pin (b) and bush (c)

## 3 Results

With the above described methods, pins and bushes of a bush chain with 8 mm pitch, which is used as a timing chain, were analyzed in both new and worn states. Furthermore, the usage of the results from these measurements as input data for the wear calculation tool is presented.

### 3.1 Initial contour

As a first step, the initial roundness and the contour of new bushes and pins were measured (see Fig. 17). With the knowledge of the initial contour of the components, the wear parameters can also be evaluated on worn components which could not be measured in the unworn state before the test run. This is often the case because disassembling and reassembling the chain could influence the wear behavior. Therefore, 10 samples of new pins and bushes were measured and analyzed.

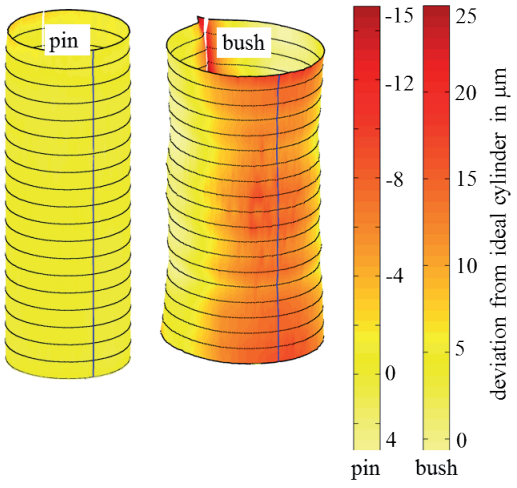


**Fig. 17** Results of roundness measurements on new pin and bush

Figure 18 shows the results for the contour of unworn bushes (Fig. 18a) and pins (Fig. 18b) with the standard deviation. Additionally, approximated contours were derived from the measurements which are also shown in the diagrams.

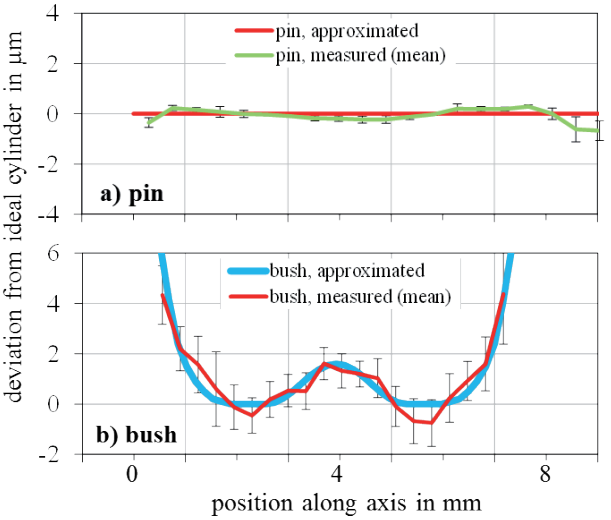


**Fig. 18** Contour of unworn pin (a) and bush (b) in the normal direction (φ=0°)

The initial shape of the bush is elliptical as explained before (see also Fig. 15). When calculating wear parameters like the maximum linear wear and the wear volume, these deviations from an ideal circle have to be taken into account. Table 1 shows the results of the initial wear parameters for pin and bush in the unworn state together with the standard deviation.

**Table 1** Initial values for linear wear and wear volume on unworn bushes and pins

| Linear wear bush $w_{maxB}$ | Wear volume bush $V_{wB}$ | Linear wear pin $w_{maxP}$ | Wear volume pin $V_{wP}$ |
|---|---|---|---|
| µm | mm³ | µm | mm³ |
| 14.1 ±2.6 | 0.236 ±0.054 | 1.0 ±0.4 | 0.001 ±0.008 |

The initial wear parameter values for new components show that the maximum linear wear on the bush is already about 14 µm while it is only 1 µm for the pin. Also the initial wear volume for the bush is 0.236 mm³ while it is close to zero for the pin. For further evaluation of the wear parameters on worn components, these initial values are subtracted from the calculation results so only the additional linear wear and wear volume are taken into account.

### 3.2 Worn Chains

The same analyses were conducted on two chains from one test run which were equipped with different types of pins (see Fig. 5).

Figure 5 shows the wear elongation for one chain joint for both chains up to a runtime of 75 h, both measured with the

wear elongation device. The wear is higher for Chain 2 with a maximum of 24 µm at the end of the runtime. The maximum wear elongation for Chain 1 is 15 µm.

The results of the roundness measurements after the post-processing are shown in Fig. 19. On the case-hardened pins from Chain 1 (Fig. 19a) a high amount of removed material can be seen while the bush shows much lower wear than the bush from Chain 2. It is obvious that the inchromized pins from Chain 2 (Fig. 19b) show almost no wear while the bush is heavily worn.

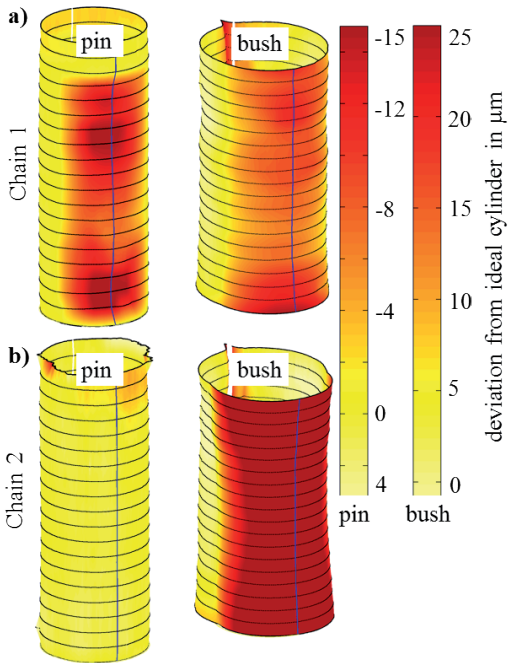


**Fig. 19** Results of roundness measurements on components of Chain 1 and Chain 2 after 75 h runtime

The wear parameters that were calculated from these measurements are presented in Table 2.

**Table 2** Wear parameters on worn bushes and pins from Chain 1 and Chain 2 including the wear elongation per chain joint from length measurement

| Parameter | Linear wear bush $w_{maxB}$ | Wear volume bush $V_{wB}$ | Linear wear pin $w_{maxP}$ | Wear volume pin $V_{wP}$ | Wear-elongation $w_{LM}$ |
|---|---|---|---|---|---|
| Unit | µm | mm³ | µm | mm³ | µm |
| Chain 1 | 5.7 ±2.6 | 0.068 ±0.054 | 15.6 ±0.4 | 0.222 ±0.008 | 15 |
| Chain 2 | 23.2 ±2.6 | 0.390 ±0.054 | 0.1 ±0.4 | -0.026 ±0.008 | 24 |

The wear parameters confirm the results from the optical assessment of the measurement data. Furthermore, the sum of the linear wear on pin and bush corresponds quite well to the wear elongation per chain joint measured with the length measurement device. The fact that the pin shows almost no wear approves that the calculation tool which only takes wear on the bush into account can be applied to at least these types of chains.

### 3.3 Usage in Simulation

As already mentioned, the initial contour of pin and bush can be used as input data for wear calculation tools. Fig. 20 shows the calculated pressure distribution for two contours of the bush while only the half of the length of the bush is shown, the other half is symmetrical. First, a cylindrical bush was used which leads to very high contact pressures at the edge of the bush. Additionally the real contour which was derived from new bushes (see Fig. 18) was used. The resulting maximum pressure is much lower and the maximum is moved towards the center of the bush. The different pressure distribution leads to a different wear behavior especially during the running-in period. After a runtime of 100 h both initial contours show the same contact pressure distribution which is almost constant along the axis of the bush.

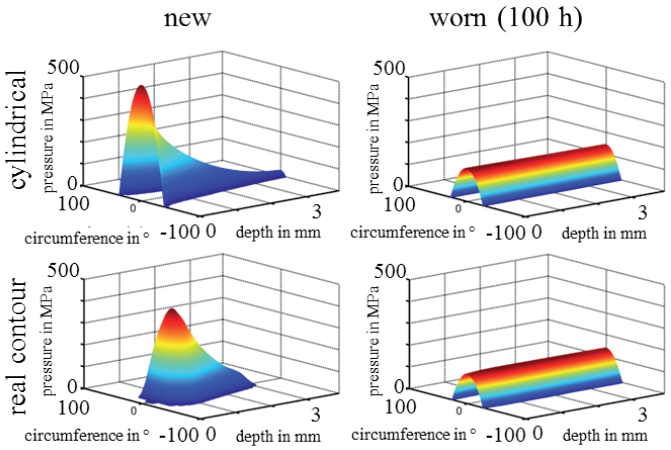


**Fig. 20** Pressure distribution for one half of the bush, calculated for a new and worn state and with a cylindrical contour and a contour that was derived from roundness measurements, 1120 N load [13]

## 4 Outlook

In the future, this method will be used to accommodate the wear investigations to gain detailed information about the wear mechanisms for different types of chains and operating conditions. Additionally the simulation methods will be improved and the roundness measurement results are used to validate the simulation results, for example by comparing the wear volume between simulation and experiment.

## 5 Conclusion

In this paper, methods for conducting wear investigations on various types of driving and timing chains are presented together with a procedure to use a standard roundness instrument to obtain the wear distribution between pin and bush and further wear parameters. The results correspond well with the results from a length measurement device. It was shown that this roundness measurement method can be used to:

- characterize new pins and bushes to compare different types of chains or manufacturing procedures
- measure the wear distribution on pin and bush and the worn contour along the axis of each component
- gain input data for calculations and simulations


## Acknowledgement

The authors would like to thank the German Research Foundation for the support of the research within the Collaborative Research Centre 926 “Microscale Morphology of Component Surfaces (MICOS)”.


## References


[1] Müller, G., Stern, D., Berlet, P., Pohlmann, K. "Praxisnahe Alterung von Motorölen und Auswirkungen auf tribologisch relevante Eigenschaften." (Practical aging of engine oils and effect on the tribologicaly relevant properties.) In: *54. Tribologie-Fachtagung (GfT) 2013, Göttingen*. 54. pp. 18/1-18/11. 2013. (In German)

[2] Polat, O., Ebrinc, A., Ozen, C., Akca, S. "*Timing Chain Wear and Effects of Different Types of Lubricants*." SAE paper: 2009-01-0198. 2009.

[3] Fink, T., Bodenstein, H. "Möglichkeiten der Reibungsreduzierung in Kettentrieben." (Potential for reducing friction in chain drives.) *MTZ – Motortechnische Zeitschrift*. 72 (7-8). pp. 582-587. 2011. (In German) DOI: 10.1365/s35146-011-0133-0

[4] Archard, J. F. "Contact and rubbing of flat surfaces." *Journal of Applied Physics*. 24 (8). pp. 981-988. 1953. DOI: 10.1063/1.1721448

[5] Gummer, A., Sappok, D., Sauer, B. "Verschleißverhalten von Hülsen- und Rollenketten." (Wear characteristics of bush and roller chains.) *ant Journal*. 4. pp. 10-16. 2013. (In German)

[6] Gummer, A. "*Analytische Untersuchung des Geometrieeinflusses auf das Verschleißverhalten von Antriebsketten*." (Analytical investigation of the geometry effect on the wear behavior of driving chains.) Ph.D. Thesis. Institute of Machine Elements, Gears, and Transmissions, University of Kaiserslautern. 2013. (In German)

[7] Sappok, D., Sauer, B. "Methoden zur Erfassung der Verschleiß-Messgrößen an Kettenkomponenten." In. *54. Tribologie-Fachtagung (GfT) 2013, Göttingen*. pp. 70/1-70/11. 2013. (In German)

[8] Sappok, D., Gummer, A., Sauer, B. "Experimental and Analytical Wear Investigations of Bush- and Roller Chain Drives." In: *5th World Tribology Congress (WTC), Torino*. 5. 2013.

[9] Lenauer, C., Wopelka, T., Jech, M., Vernes, A. "Influence of Tribological Parameters on Wear Behaviour." In: *5th World Tribology Congress (WTC), Torino*. 5. 2013.

[10] Bayer, R. G. "*Mechanical wear prediction and prevention*." New York, Marcel Dekker Inc. 1994.

[11] ISO 12180-2: Geometrical product specifications (GPS) - Cylindricity - Part 2: Specification operators. 2011.

[12] Smith, G. T. "*Industrial metrology: Surfaces and roundness*." London, New York, Springer. 2002.

[13] Sappok, D., Merz, R. M., Sauer, B., Kopnarski, M. "Surface Analysis of Chain Joint Components after Tribological Load and Usage of Anti-wear Additives." In: *Conference Papers in Science - European Symposium on Friction, Wear, and Wear Protection*. Article ID 407048. 2014.